

The NLO twist-3 contributions to $B \rightarrow \pi$ form factors in k_T factorization

Shan Cheng¹, Ying-Ying Fan¹, Xin Yu², Cai-Dian Lü^{2,*} and Zhen-Jun Xiao^{1,†}

1. *Department of Physics and Institute of Theoretical Physics,
Nanjing Normal University, Nanjing, Jiangsu 210023, People's Republic of China, and*

2. *Institute of High Energy Physics and Theoretical Physics Center for Science Facilities,
Chinese Academy of Sciences, Beijing 100049, People's Republic of China,*

(Dated: February 28, 2014)

In this paper, we calculate the next-to-leading-order (NLO) twist-3 contribution to the form factors of $B \rightarrow \pi$ transitions by employing the k_T factorization theorem. All the infrared divergences regulated by the logarithms $\ln(k_{iT}^2)$ cancel between those from the quark diagrams and from the effective diagrams for the initial B meson wave function and the final pion meson wave function. An infrared finite NLO hard kernel is therefore obtained, which confirms the application of the k_T factorization theorem to B meson semileptonic decays at twist-3 level. From our analytical and numerical evaluations, we find that the NLO twist-3 contributions to the form factors $f^{+,0}(q^2)$ of $B \rightarrow \pi$ transition are similar in size, but have an opposite sign with the NLO twist-2 contribution, which leads to a large cancelation between these two NLO parts. For the case of $f^+(0)$, for example, the 24% NLO twist-2 enhancement to the full LO prediction is largely canceled by the negative (about -17%) NLO twist-3 contribution, leaving a small and stable 7% enhancement to the full LO prediction in the whole range of $0 \leq q^2 \leq 12 \text{ GeV}^2$. At the full NLO level, the perturbative QCD prediction is $F^{B \rightarrow \pi}(0) = 0.269^{+0.054}_{-0.050}$.

I. INTRODUCTION

Without end-point singularity, k_T factorization theorem [1–3] is a better tool to deal with the small x physics when comparing with other factorization approaches[4–8]. Based on the k_T factorization theorem, perturbative QCD (pQCD) factorization approach[9–12] is a successful factorization approach to handle the heavy to light exclusive decay processes. As an effective factorization theorem, the k_T factorization should be valid at every order expanded by strong coupling $O(\alpha_s^n)$, where n is the power of the expansion.

Recently, the next-to-leading-order(NLO) twist-2 (the leading twist) contributions to the form factors for the $\pi\gamma^* \rightarrow \gamma$, $\pi\gamma^* \rightarrow \pi$ and $B \rightarrow \pi$ transitions have been evaluated [13–15] by employing the k_T factorization theorem [1–3], and an infrared finite k_T dependent hard kernel were obtained at the NLO level for each considered process. It is worth of mentioning that a new progress about pion form factor in the $\pi\gamma^* \rightarrow \gamma$ scattering has been made in Ref. [16] very recently, where the authors made a joint resummation for the pion wave function and the pion transition form factor and proved that the k_T factorization is scheme independent. These NLO contributions could produce sizable effects to the LO hard kernels. For example, the NLO twist-2 contribution to the form factor $F_0^{B \rightarrow \pi}(0)$ for $B \rightarrow \pi$ transition can provide $\sim 30\%$ enhancement to the corresponding full LO form factor [15]. In a recent paper [17], we calculated the NLO

* lucd@ihep.ac.cn

† xiaozhenjun@njnu.edu.cn

twist-3 contribution to the pion electromagnetic form factor $F_{\pi\gamma}(Q^2)$ in the $\pi\gamma^* \rightarrow \pi$ process by employing the k_T factorization theorem, and found infrared finite NLO twist-3 corrections to the full LO hard kernels [17].

In this paper, following the same procedure of Ref. [15], we will calculate the NLO twist-3 contribution to the form factor of $B \rightarrow \pi$ transition, which is the only missing piece at the NLO level. The light partons are also considered to be off-shell by k_T^2 in both QCD quark diagrams and effective diagrams for hadron wave functions. The radiation gluon from the massive b quark generates the soft divergence only. Such soft divergence can be regulated either by the virtuality of internal particles or by the virtuality k_T^2 of other light partons, to which the emission gluons were attached. So we can replace the off-shell scale k_T^2 for the light parton by m_g for the massive b quark safely to regulate the IR divergences from the massive b quark line, where m_g means the mass of the gluon radiated from the b quark. That means, the b quark remains on-shell in the framework.

We will prove that the IR divergences in the NLO QCD quark diagrams could be canceled by those in the effective diagrams, i.e., the convolution of the $O(\alpha_s)$ B meson and π meson wave functions with the LO hard kernel. The IR finiteness and k_T -dependent NLO hard kernel were also derived at the twist-3 level for the $B \rightarrow \pi$ transition form factor, which confirms the application of the k_T factorization theorem to B meson semileptonic decays at both the twist-2 and twist-3 level.

In our calculation for the NLO twist-3 contribution, the resummation technology[18, 19] is applied to deal with the large double logarithms $\alpha_s \ln^2 k_T$ and $\alpha_s \ln^2 x_i$, where x_i being the parton momentum fraction of the anti-quark in the meson wave functions. With appropriate choices of μ and μ_f , say being lower than the B meson mass, the NLO corrections are under control. From numerical evaluations we find that the NLO correction at twist-3 is about -17% of the LO part, while the NLO twist-2 contribution can provide a 24% enhancement to the LO one. This means that the NLO twist-2 contribution to the form factor $F^{B \rightarrow \pi}(0)$ are largely canceled by the NLO twist-3 one, leaves a net small correction to the full LO form factor, around or less than 7% enhancement.

The paper is organized as follows. In Sec. II, we give a brief introduction for the calculations of the LO diagrams relevant with the form factor of $B \rightarrow \pi$ transition. In Sec. III, we calculate the NLO twist-3 contribution to the $B \rightarrow \pi$ form factor. The relevant $O(\alpha_s^2)$ QCD quark diagrams are calculated analytically, the convolutions of $O(\alpha_s)$ wave functions and $O(\alpha_s)$ hard kernel are made in the same way as those for the evaluation of the NLO twist-2 contribution. And finally we extract out the expression of the factor $F_{\text{NLO-T3}}^{B \rightarrow \pi}(x_i, \mu, \mu_f, \eta)$, which describes the NLO twist-3 contribution to the form factor $F^{B \rightarrow \pi}(x_i, \mu, \mu_f, \eta)$. In Sec. IV we calculate and present the numerical results for the relevant form factors and examine the q^2 -dependence of $F^+(q^2)$ and $F^0(q^2)$ at the LO and NLO level, respectively. A short summary was given in the final section.

II. LO ANALYSIS

By employing the k_T factorization theorem, the LO twist-2 and twist-3 contributions to the form factor of $B \rightarrow \pi$ transition have been calculated many years ago [9–12]. For the sake of the readers, we here present the expressions of the leading order hard kernels directly.

The $B \rightarrow \pi$ transition form factors are defined via the matrix element

$$\langle \pi(p_2) | \bar{u} \gamma^\mu b | B(p_1) \rangle = f^+(q^2)(p_1^\mu + p_2^\mu) + [f^0(q^2) - f^+(q^2)] \frac{m_B^2 - m_\pi^2}{q^2} q^\mu, \quad (1)$$

where m_B (m_π) is the B (π) meson mass, and $q = p_1 - p_2$ is the transfer momentum. The

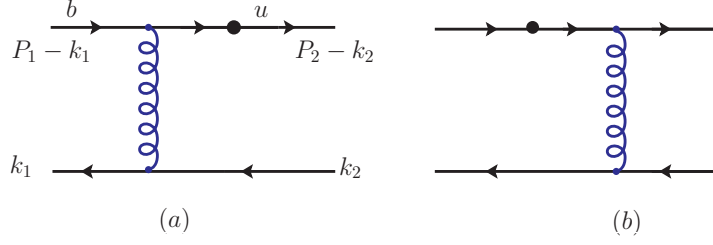


FIG. 1. Leading-order quark diagrams for the $B \rightarrow \pi$ transition form factor with symbol \bullet representing the weak vertex of $B \rightarrow \pi l \bar{\nu}_l$ decay.

momentum p_1 (p_2) is chosen as $p_1 = p_1^+(1, 1, \mathbf{0}_T)$ ($p_2 = (0, p_2^-, \mathbf{0}_T)$) with the component $p_1^+ = m_B/\sqrt{2}$ and $p_2^- = \eta m_B/\sqrt{2}$. Here the parameter $\eta = 1 - q^2/m_B^2$ represents the energy fraction carried by the pion meson, and $\eta \sim O(1)$ when in the large recoil region of pion. According to the k_T factorization, the anti-quark \bar{q} carries momentum $k_1 = (x_1 p_1^+, 0, \mathbf{k}_{1T})$ in the B meson and $k_2 = (0, x_2 p_2^-, \mathbf{k}_{2T})$ in the pion meson as labeled in Fig. 1, x_1 and x_2 being the momentum fractions. The follow hierarchy is postulated in the small- x region:

$$m_B^2 \gg x_2 m_B^2 \gg x_1 m_B^2 \gg x_1 x_2 m_B^2, k_{1T}^2, k_{2T}^2, \quad (2)$$

which is roughly consistent with the order of magnitude: $x_1 \sim 0.1$, $x_2 \sim 0.3$, $m_B \sim 5$ GeV, and $k_T \lesssim 1$ GeV [15].

The LO hard kernels are obtained after sandwiching Fig. 1 with the B meson and the pion meson wave functions[9, 10, 20]

$$\Phi_B(x_1, p_1) = \frac{1}{2\sqrt{N_c}} (\not{p}_1 + m_B) \gamma_5 \left[\not{\epsilon}_+ \phi_B^+(x_1) + \left(\not{\epsilon}_- - k_1^+ \gamma_\perp^\nu \frac{\partial}{\partial \mathbf{k}_{1T}^\nu} \right) \phi_B^-(x_1) \right], \quad (3)$$

$$\Phi_\pi^{T2}(x_2, p_2) = \frac{1}{\sqrt{2N_c}} \gamma_5 \not{p}_2 \phi_\pi^A(x_2), \quad (4)$$

$$\Phi_\pi^{T3}(x_2, p_2) = \frac{1}{\sqrt{2N_c}} m_0 \gamma_5 [\phi_\pi^P(x_2) - (\not{\epsilon}_- \not{\epsilon}_+ - 1) \phi_\pi^T(x_2)], \quad (5)$$

where m_0 is the chiral mass of pion, Φ_π^{T2} and Φ_π^{T3} denote the pion meson wave function at twist-2 and twist-3 level, the dimensionless vectors are defined by $\not{\epsilon}_+ = (1, 0, \mathbf{0}_T)$, and $\not{\epsilon}_- = (0, 1, \mathbf{0}_T)$, and N_c is the number of colors. Without considering the transverse component of the B meson spin projector, the LO twist-3 contribution for Fig. 1(a) is of the form,

$$H_{a,T3}^{(0)}(x_1, k_{1T}, x_2, k_{2T}) = g_s^2 C_F m_0 m_B \phi_B^+(x_1) \cdot \frac{\phi_\pi^P(x_2) (4p_1^\mu - 8x_2 p_2^\mu) + \phi_\pi^T(x_2) \left[-4p_1^\mu + 4p_2^\mu \left(\frac{2}{\eta} - 2x_2 \right) \right]}{[(p_1 - k_2)^2 - m_B^2][(k_1 - k_2)^2]}, \quad (6)$$

where the approximation $\phi_B^+ = \phi_B^-$ [21, 22] has been taken, and for Fig. 1(b) we find

$$H_{b,T3}^{(0)}(x_1, k_{1T}, x_2, k_{2T}) = 2g_s^2 C_F m_0 m_B \phi_\pi^P(x_2) \frac{4p_2^\mu \phi_B^+(x_1) - 4x_1 p_1^\mu \phi_B^-(x_1)}{[(p_2 - k_1)^2][(k_1 - k_2)^2]}, \quad (7)$$

where $C_F = 4/3$ is the color factor.

The LO twist-2 contributions for Fig. 1(a) and 1(b) are of the form,

$$H_{a,T2}^{(0)}(x_1, k_{1T}, x_2, k_{2T}) = -4g_s^2 C_F m_B^2 \phi_\pi^A(x_2) \frac{p_2^\mu \phi_B^-(x_1) + k_2^\mu \phi_B^+(x_1)}{[(p_1 - k_2)^2 - m_B^2][(k_1 - k_2)^2]}, \quad (8)$$

$$H_{b,T2}^{(0)}(x_1, k_{1T}, x_2, k_{2T}) = -4g_s^2 C_F m_B^2 \phi_\pi^A(x_2) x_1 \frac{(\eta p_1^\mu - p_2^\mu) \phi_B^+(x_1) + p_2^\mu \phi_B^-(x_1)}{[(p_2 - k_1)^2][(k_1 - k_2)^2]}. \quad (9)$$

For the LO twist-2 hard kernel $H_{b,T2}^{(0)}$, it is strongly suppressed by the small x_2 , as can be seen easily from Eqs. (8,9), and therefore the $H_{a,T2}^{(0)}$ from Fig. 1(a) is the dominant part of the full LO twist-2 contribution. Consequently, it is reasonable to consider the NLO twist-2 contributions from Fig. 1(a) only in the calculation for the NLO twist-2 contributions.

For the LO twist-3 hard kernel $H_{b,T3}^{(0)}$, the first term proportional to $p_2^\mu \phi_B^+(x_1)$ in Eq. (7) provides the dominant contribution, while the second term proportional to $x_1 p_1^\mu \phi_B^0(x_1)$ is strongly suppressed by the small x_1 . The $H_{a,T3}^{(0)}$ can be neglected safely when compared with $H_{b,T3}^{(0)}$, due to the strong suppression of small x_1 and the cancelation between the terms proportional to $\phi_\pi^P(x_2)$ and $\phi_\pi^T(x_2)$. We therefore consider only the $\phi_\pi^P(x_2)$ component in Eq. (7) from Fig. 1(b) in our estimation for the NLO twist-3 contribution.

The LO hard kernels as given in Eqs.(6-9) are consistent with those as given in Refs. [21, 22], where the B meson wave function was defined as

$$-\frac{1}{\sqrt{2N_c}} (\not{p}_1 + m_B) \gamma_5 [\phi_B(x_1) - \frac{\not{p}_+ - \not{p}_-}{\sqrt{2}} \bar{\phi}_B(x_1)], \quad (10)$$

with the relations

$$\phi_B = \frac{1}{2}(\phi_B^+ + \phi_B^-), \quad \bar{\phi}_B = \frac{1}{2}(\phi_B^+ - \phi_B^-). \quad (11)$$

By comparing the hard kernel $H_{b,T3}^{(0)}$ in Eq. (7) with $H_{a,T2}^{(0)}$ in Eq. (8), one can find that the LO twist-3 contribution is enhanced by the factor $1/x_1$ and the pion chiral mass $M_0 > 1$, and which is larger than the LO twist-2 contribution which are associated with the factor $1/x_2$. The numerical results of Eq. (7,8) in the large recoil region also show that the LO twist-3 contribution is larger than the LO twist-2 part, by a ratio of around 60% over 40%. This fact means that the NLO twist-3 contribution may be important when compared with the corresponding NLO twist-2 one, this is one of the motivations for us to make the evaluation for the NLO twist-3 contribution to the $B \rightarrow \pi$ form factor.

III. NLO CORRECTIONS

Since the dominant NLO twist-3 contribution to the form factor of $B \rightarrow \pi$ transition is proportional to the $\phi_\pi^P(x_2) \phi_B^+(x_1)$ from the Fig. 1(b), we here consider only the NLO corrections to the Fig. 1(b) coming from the quark-level corrections and the wave function corrections at twist-3 level, to find the NLO twist-3 contribution to the form factor of $B \rightarrow \pi$ transition.

Under the hierarchy in Eq. (2), only terms that don't vanish in the limits of $x_i \rightarrow 0$ and $k_{iT}^2 \rightarrow 0$ are kept to simplify the expressions of the NLO twist-3 contributions greatly.

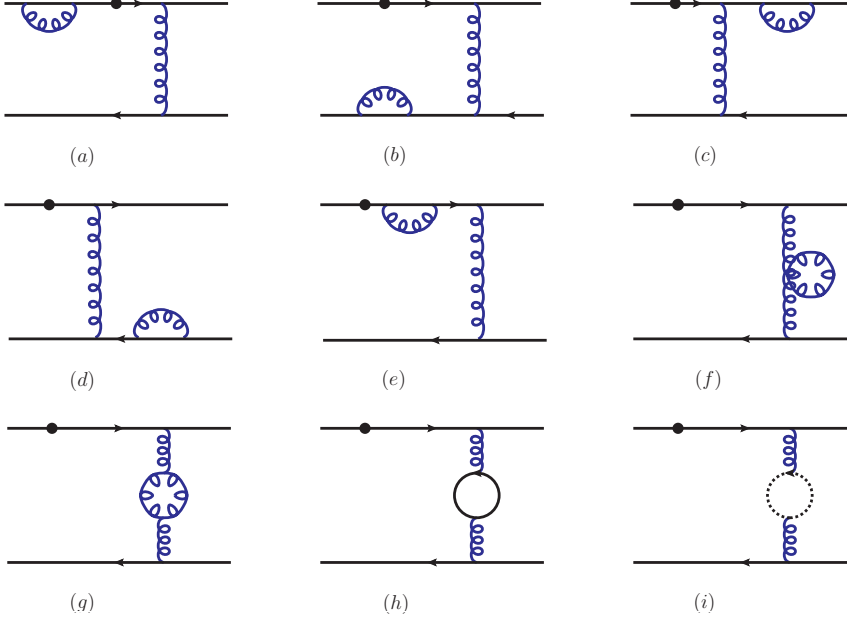


FIG. 2. Self-energy corrections to fig.1(b).

A. NLO Corrections from the QCD Quark Diagrams

The NLO corrections to Fig. 1(b) at quark-level contain the self-energy diagrams, the vertex diagrams and the box and pentagon diagrams, as illustrated by Fig. 2, 3, 4, respectively. The ultra-violet(UV) divergences are extracted in the dimensional reduction[23] in order to avoid the ambiguity from handling the matrix γ_5 . The infrared(IR) divergences are identified as the logarithms $\ln m_g$, $\ln \delta_1$, $\ln \delta_2$ and their combinations, where the dimensionless ratios are adopted,

$$\delta_1 = \frac{k_{1T}^2}{m_B^2}, \quad \delta_2 = \frac{k_{2T}^2}{m_B^2}, \quad \delta_{12} = \frac{-(k_1 - k_2)^2}{m_B^2}, \quad (12)$$

By analytical evaluations for the Feynman diagrams as shown in Fig. 2, we find the self-energy corrections from the nine diagrams:

$$G_{2a}^{(1)} = -\frac{\alpha_s C_f}{4\pi} \left[\frac{6}{\delta_1} \left(\frac{1}{\epsilon} + \ln \frac{4\pi\mu^2}{m_B^2 e^{\gamma_E}} + \frac{1}{3} \right) + \frac{1}{2} \left(\frac{1}{\epsilon} + \ln \frac{4\pi\mu^2}{m_B^2 e^{\gamma_E}} + 2 \ln \frac{m_g^2}{m_B^2} + 2 \right) \right] H^{(0)}, \quad (13)$$

$$G_{2b}^{(1)} = -\frac{\alpha_s C_f}{8\pi} \left[\frac{1}{\epsilon} + \ln \frac{4\pi\mu^2}{\delta_1 m_B^2 e^{\gamma_E}} + 2 \right] H^{(0)}, \quad (14)$$

$$G_{2c,2d}^{(1)} = -\frac{\alpha_s C_f}{8\pi} \left[\frac{1}{\epsilon} + \ln \frac{4\pi\mu^2}{\delta_2 m_B^2 e^{\gamma_E}} + 2 \right] H^{(0)}, \quad (15)$$

$$G_{2e}^{(1)} = -\frac{\alpha_s C_f}{4\pi} \left[\frac{1}{\epsilon} + \ln \frac{4\pi\mu^2}{x_1 \eta m_B^2 e^{\gamma_E}} + 2 \right] H^{(0)}, \quad (16)$$

$$G_{2f+2g+2h+2i}^{(1)} = \frac{\alpha_s}{4\pi} \left[\left(\frac{5}{3} N_c - \frac{2}{3} N_f \right) \left(\frac{1}{\epsilon} + \ln \frac{4\pi\mu^2}{\delta_{12} m_B^2 e^{\gamma_E}} \right) \right] H^{(0)}, \quad (17)$$

where $1/\epsilon$ represents the UV pole, μ is the renormalization scale, γ_E is the Euler constant, N_c is the number of quark color, N_f is the number of the quarks flavors, and $H^{(0)}$ denotes the first term

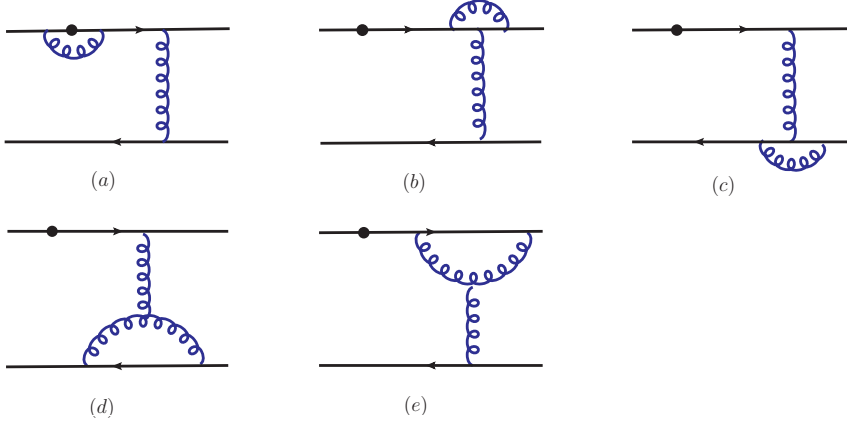


FIG. 3. Vertex corrections to fig.1(b).

of the LO twist-3 contribution $H_{b,T3}^{(0)}(x_1, k_{1T}, x_2, k_{2T})$ as given in Eq. (7),

$$H^{(0)}(x_1, k_{1T}, x_2, k_{2T}) = -4g_s^2 C_F m_0 m_B \phi_\pi^P(x_2) \frac{2p_2^\mu \phi_B^+(x_1)}{(p_2 - k_1)^2 (k_1 - k_2)^2}. \quad (18)$$

It's easy to see that, besides $G_{2e}^{(1)}$ for the subdiagram Fig. 2(e), the NLO self-energy corrections listed in Eqs. (14,15,17) are identical to the self-energy corrections for the NLO twist-2 case as given in Eqs. (7-8,11) in Ref. [15]. Except for a small difference in constant numbers, the $G_{2a}^{(1)}$ for the subdiagram Fig. 2(a) in Eq. (13) is the same one as that as given in Eq. (7) of Ref. [15] for the case of the NLO twist-2 contributions. The reason for such high similarity is that the self-energy diagrams don't involve the loop momentum flowed into the hard kernel. Only the Fig. 2(a), the self-energy correction of the b quark is emphasized here. The first term in the square brackets of $G_{2a}^{(1)}$ required the mass renormalization, and the finite piece of the first term is then absorbed into the redefinition the b quark mass, with the relation $(p_1 - k_1)^2 - m_B^2 = -k_{1T}^2$. The second term in the square brackets of $G_{2a}^{(1)}$ represents the correction to the b quark wave function. The involved soft divergence is regularized by the gluon mass m_g because the valence b quark is considered on-shell, and the additional regulator m_g will be canceled by the corresponding soft divergence in the effective diagrams Fig. 5(a). Comparing with the NLO twist-2 case, the result from the subdiagram Fig. 2(e) at twist-3 is simple, since it's the self-energy correction to the massless internal quark line in the twist-3 case.

By analytical evaluations for the Feynman diagrams as shown in Fig. 3, we find the vertex corrections from the five vertex diagrams:

$$G_{3a}^{(1)} = \frac{\alpha_s C_F}{4\pi} \left[\frac{1}{\epsilon} + \ln \frac{4\pi\mu^2}{m_B^2 e^{\gamma_E}} - \ln^2 x_1 - 2 \ln x_1 (1 - \ln \eta) - \frac{2\pi^2}{3} - 1 \right] H^{(0)}, \quad (19)$$

$$G_{3b}^{(1)} = -\frac{\alpha_s}{8\pi N_c} \left[\frac{1}{\epsilon} + \ln \frac{4\pi\mu^2}{x_1 \eta m_B^2 e^{\gamma_E}} - \frac{1}{2} \right] H^{(0)}, \quad (20)$$

$$G_{3c}^{(1)} = -\frac{\alpha_s}{8\pi N_c} \left[\frac{1}{\epsilon} + \ln \frac{4\pi\mu^2}{\delta_{12} m_B^2 e^{\gamma_E}} - \ln \frac{\delta_2}{\delta_{12}} \ln \frac{\delta_1}{\delta_{12}} - \ln \frac{\delta_1 \delta_2}{\delta_{12}^2} - \frac{\pi^2}{3} \right] H^{(0)}, \quad (21)$$

$$G_{3d}^{(1)} = \frac{\alpha_s N_c}{8\pi} \left[\frac{3}{\epsilon} + 3 \ln \frac{4\pi\mu^2}{\delta_{12} m_B^2 e^{\gamma_E}} - \ln \frac{\delta_1 \delta_2}{\delta_{12}^2} + \frac{11}{2} - \frac{2\pi^2}{3} \right] H^{(0)}, \quad (22)$$

$$G_{3e}^{(1)} = \frac{\alpha_s N_c}{8\pi} \left[\frac{3}{\epsilon} + 3 \ln \frac{4\pi\mu^2}{x_1 \eta m_B^2 e^{\gamma_E}} - \ln \frac{\delta_2}{x_1 \eta} (\ln x_2 + 1) + \frac{1}{2} \ln x_2 - \frac{\pi^2}{3} + \frac{7}{4} \right] H^{(0)}. \quad (23)$$

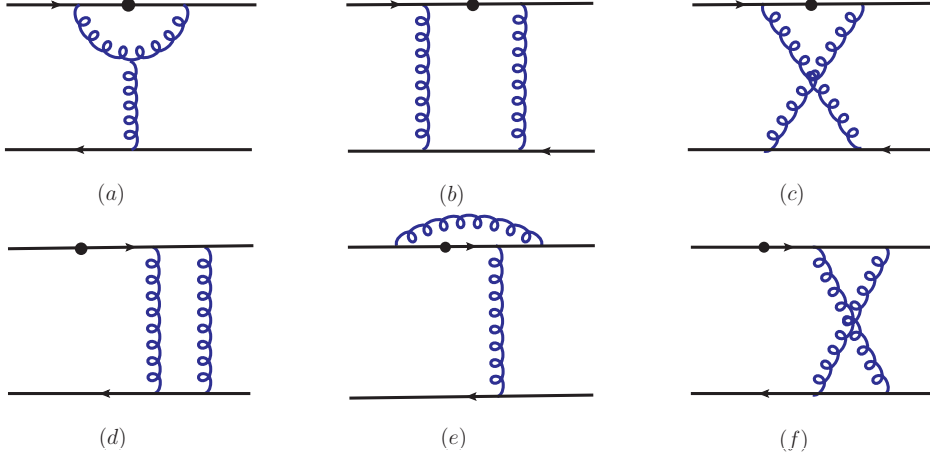


FIG. 4. Box and pentagon corrections to fig.1(b).

The amplitude $G_{3a}^{(1)}$ have no IR divergence due to the fact that the radiative gluon attaches to the massive b quark and the internal line in Fig. 3(a). The amplitude $G_{3b}^{(1)}$ should have collinear divergence at the first sight because the radiative gluon in Fig. 3(b) attaches to the light valence quark, but it's found that the collinear region $l \parallel p_2$ was suppressed, then $G_{3b}^{(1)}$ is IR finite. The radiative gluon in Fig. 3(c) attaches to the light valence anti-quarks, so that both the collinear and soft divergences are produced in $G_{3c}^{(1)}$, where the large double logarithm $\ln \delta_1 \ln \delta_2$ denoted the overlap of the IR divergences can be absorbed into the B meson or the pion meson wave functions. The radiative gluon in Fig. 3(d) attaches to the light valence anti-quarks as well as the virtual LO hard gluon, so the soft divergence and the large double logarithm aren't generated in $G_{3d}^{(1)}$. The radiative gluon in Fig. 3(e) attaches only to the light valence quark as well as the virtual LO hard gluon, and then $G_{3e}^{(1)}$ just contains the collinear divergence regulated by $\ln \delta_2$ from $l \parallel p_2$ region.

The analytical results from the box and pentagon diagrams as shown in Fig. 4 are summarized as

$$G_{4a}^{(1)} = -\frac{\alpha_s N_c}{8\pi} x_1 \left[\ln \frac{x_2 \eta^2}{\delta_2} + 1 \right] H^{(0)}, \quad (24)$$

$$G_{4b}^{(1)} = -\frac{\alpha_s C_f}{4\pi} \left[\ln^2 \frac{\delta_1}{x_1^2} - \ln^2 x_1 - \frac{7\pi^2}{3} \right] H^{(0)}, \quad (25)$$

$$G_{4c}^{(1)} = -\frac{\alpha_s}{8\pi N_c} \left[\ln \frac{\delta_1}{\delta_{12}} \ln \frac{\delta_2}{\delta_{12}} - \frac{\pi^2}{12} \right] H^{(0)}, \quad (26)$$

$$G_{4d}^{(1)} = -\frac{\alpha_s C_F}{2\pi} \left[\ln \frac{\delta_1}{\delta_{12}} \ln \frac{\delta_2}{\delta_{12}} + \frac{\pi^2}{3} \right] H^{(0)}, \quad (27)$$

$$G_{4e}^{(1)} = \frac{\alpha_s}{8\pi N_c} \left[\ln \frac{\delta_1}{\eta} \ln \frac{\delta_2}{\eta} + \ln \delta_2 + \frac{\pi^2}{6} \right] H^{(0)}, \quad (28)$$

$$G_{4f}^{(1)} = -\frac{\alpha_s}{8\pi N_c} \left[\ln \frac{\delta_1}{\eta} \ln \frac{\delta_2}{\eta} - \ln x_2 \ln \delta_2 - \ln x_2 \ln \delta_{12} \right. \\ \left. + \frac{1}{2} \ln^2 \eta + \frac{1}{2} \ln^2 \delta_{12} - \frac{1}{2} \ln^2 x_2 - \frac{\pi^2}{3} - 1 \right] H^{(0)}. \quad (29)$$

Note that the amplitude of Fig. 4(a) has no IR divergence because the additional gluon is linked to the massive b quark and the virtual LO hard kernel gluon. Fig. 4(b) is two-particle reducible,

whose IR contribution would be canceled by the corresponding effective diagrams for the B meson function Fig. 5(c). All the other four subdiagrams Fig. 5(c,d,e,f) would generate double logarithms from the overlap region of the soft and collinear region, because the radiative gluon attached with b quark and light valence quark generate both collinear divergence and soft divergence, as well as the gluon attached two light valence partons. Fig. 4(d) is also a two-particle reducible diagram, whose contribution should be canceled completely by the corresponding effective diagrams Fig. 5(c) for the pion meson function due to the requirement of the factorization theorem. It's found that the double logarithm in Fig. 4(c) offset with the double logarithm in Fig. 3(c), and the cancelation would also appear for the double logarithms in Fig. 4(e) and Fig. 4(f).

The NLO twist-3 corrections from all the three kinds of the QCD quark diagrams are summed into

$$\begin{aligned}
G^{(1)} = \frac{\alpha_s C_f}{4\pi} & \left\{ \frac{21}{4} \left(\frac{1}{\epsilon} + \ln \frac{4\pi\mu^2}{m_B^2 e^{\gamma_E}} \right) - \ln^2 \delta_1 - 2 \ln \delta_1 \ln \delta_2 - \frac{97}{16} \ln^2 x_1 - \frac{15}{8} \ln^2 x_2 \right. \\
& + \frac{1}{2} (-1 + 12 \ln x_1 + 4 \ln x_2 + 4 \ln \eta) \ln \delta_1 + (-1 + 2 \ln x_1 + \ln x_2 + 2 \ln \eta) \ln \delta_2 \\
& - \frac{23}{8} \ln x_1 \ln x_2 - \frac{1}{8} (41 + 17 \ln \eta) \ln x_1 - \frac{1}{16} (41 + 46 \ln \eta) \ln x_2 \\
& \left. - \frac{1}{96} [-273 + \pi^2 + 96 \ln r_g + 12 \ln \eta (25 + 17 \ln \eta)] \right\} H^{(0)}, \quad (30)
\end{aligned}$$

for $N_f = 6$. The UV divergence in the above expression is the same as in the pion electromagnetic form factor[14] and in the leading twist of $B \rightarrow \pi$ transition form factor[15], which determines the renormalization-group(RG) evolution of the coupling constant α_s . The double logarithm arose from the reducible subdiagrams Fig. 4(b,d) would be absorbed into the NLO wave functions.

B. NLO Corrections of the Effective Diagrams

As point out in Ref. [15], a basic argument of k_T factorization is that the IR divergences arisen from the NLO corrections can be absorbed into the non-perturbative wave functions which are universal. From this point, the convolution of the NLO wave function $\Phi_B^{(1)}$ and the LO hard kernel $H^{(0)}$, the LO hard kernel $H^{(0)}$ and the NLO wave function $\Phi_\pi^{(1)}$ are computed, and then to cancel the IR divergences in the NLO amplitude $G^{(1)}$ as given in Eq. (30). The convolutions for NLO wave functions and LO hard kernel are calculated in this subsection. In k_T factorization theorem, the $\Phi_B^{(1)}$ [24] collect the $O(\alpha_s)$ effective diagrams from the matrix elements of the leading Fock states $\Phi_B(x_1, k_{1T}; x'_1, k'_{1T})$, and $\Phi_{\pi,P}^{(1)}$ collect the $O(\alpha_s)$ effective diagrams for the twist-3 transverse momenta dependent (TMD) light-cone wave function $\Phi_{\pi,P}(x_2, k_{2T}; x'_2, k'_{2T})$ [25, 26]

$$\begin{aligned}
\Phi_B(x_1, k_{1T}; x'_1, k'_{1T}) &= \int \frac{dz^-}{2\pi} \frac{d^2 z_T}{(2\pi)^2} e^{-ix'_1 P_1^+ z^- + i\mathbf{k}'_{1T} \cdot \mathbf{z}_T} \\
&\cdot \langle 0 | \bar{q}(z) W_z(n_1)^\dagger I_{n_1; z, 0} W_0(n_1) \not{n}_+ \Gamma h_\nu(0) | h_\nu \bar{d}(k_1) \rangle, \quad (31)
\end{aligned}$$

$$\begin{aligned}
\Phi_{\pi,P}(x_2, k_{2T}; x'_2, k'_{2T}) &= \int \frac{dy^+}{2\pi} \frac{d^2 y_T}{(2\pi)^2} e^{-ix'_2 P_2^- y^+ + i\mathbf{k}'_{2T} \cdot \mathbf{y}_T} \\
&\cdot \langle 0 | \bar{q}(y) W_y(n_2)^\dagger I_{n_2; y, 0} W_0(n_2) \gamma_5 q(0) | u(p_2 - k_2) \bar{d}(k_2) \rangle, \quad (32)
\end{aligned}$$

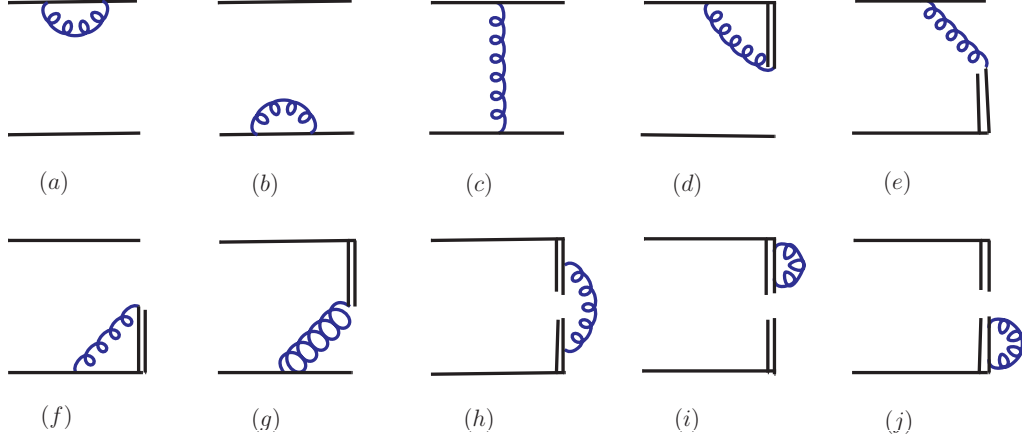


FIG. 5. $O(\alpha_s)$ diagrams for the B meson function.

respectively, in which $z = (0, z_-, \mathbf{z}_T)$ and $y = (y^+, 0, \mathbf{y}_T)$ are the light cone (LC) coordinates of the anti-quark field \bar{d} carried the momentum fraction x_i respectively, and h_ν is the effective heavy-quark field.

$$W_z(n_1) = \text{P exp} \left[-ig_s \int_0^\infty d\lambda n_1 \cdot A(z + \lambda n_1) \right], \quad (33)$$

$$W_y(n_2) = \text{P exp} \left[-ig_s \int_0^\infty d\lambda n_2 \cdot A(y + \lambda n_2) \right], \quad (34)$$

where P is the path ordering operator. The two Wilson line $W_{y/z}(n_i)$ and $W_0(n_i)$ are connected by a vertical link $I_{n_i; y/z, 0}$ at infinity[27]. Then the additional LC singularities from the region where loop momentum $l \parallel n_-(n_+)$ [28] are regulated by the IR regulator n_1^2 and n_2^2 . The scales $\xi_1^2 \equiv 4(n_1 \cdot p_1)^2/|n_1^2| = m_B^2|n_1^-/n_1^+|$ and $\xi_2^2 \equiv 4(n_2 \cdot p_2)^2/|n_2^2| = \eta^2 m_B^2|n_2^+/n_2^-|$ are introduced to avoid the LC singularity[15, 29]. It's important to emphasize that the variation of the above scales is regarded as a factorization scheme-dependence, which would be brought into the NLO hard kernel after taking the difference between the QCD quark diagrams and the effective diagrams. And the above scheme-dependent scales can be minimized by adhering to fixed n_1^2 and n_2^2 . In Ref. [30], very recently, Li et al. studied the joint resummation for pion wave function and pion transition form factor, i.e., summing up the mixed logarithm $\ln(x_i) \ln(k_T)$ to all orders. Such joint resummation can reduce the above scheme dependence effectively.

The convolution for $O(\alpha_s)$ order of B meson function in Eq. (31) and $H^{(0)}$ over the integration variables x'_1 and k'_{1T} is

$$\Phi_B^{(1)} \otimes H^{(0)} \equiv \int dx'_1 d^2 \mathbf{k}'_{1T} \Phi_B^{(1)}(x_1, \mathbf{k}_{1T}; x'_1, \mathbf{k}'_{1T}) H^{(0)}(x'_1, \mathbf{k}'_{1T}; x_2, \mathbf{k}_{2T}). \quad (35)$$

In the evolution, the n_1 is approximated to vector n_- with a very small plus component n_1^+ to avoid the LC singularity in the integration, and we choose n_1^- to be positive while n_1^+ can be positive or negative for convenience. The NLO twist-3 corrections from the $O(\alpha_s)$ order wave function as

shown in Fig. 5 are listed in the following with μ_f being the factorization scale:

$$\Phi_{5a}^{(1)} \otimes H^{(0)} = \frac{\alpha_s C_f}{4\pi} \left[\frac{1}{\epsilon} + \ln \frac{4\pi\mu_f^2}{m_B^2 e^{\gamma_E}} - \ln r_g \right] H^{(0)}, \quad (36)$$

$$\Phi_{5b}^{(1)} \otimes H^{(0)} = -\frac{\alpha_s C_f}{8\pi} \left[\frac{1}{\epsilon} + \ln \frac{4\pi\mu_f^2}{m_B^2 e^{\gamma_E}} - \ln \delta_1 + 2 \right] H^{(0)}, \quad (37)$$

$$\Phi_{5c}^{(1)} \otimes H^{(0)} = -\frac{\alpha_s C_f}{4\pi} \left[\ln^2 \left(\frac{\delta_1}{x_1^2} \right) \right] H^{(0)}, \quad (38)$$

$$\Phi_{5d}^{(1)} \otimes H^{(0)} = -\frac{\alpha_s C_f}{8\pi} (-\ln r_1) \left[\frac{1}{\epsilon} + \ln \frac{4\pi\mu_f^2}{m_B^2 e^{\gamma_E}} - \ln r_g \right] H^{(0)}, \quad (39)$$

$$\Phi_{5e}^{(1)} \otimes H^{(0)} = \frac{\alpha_s C_f}{4\pi} (-\ln r_1) \left[-\ln r_1 - \ln r_g + \frac{1}{2} \ln r_1 + 2 \ln x_1 \right] H^{(0)}, \quad (40)$$

$$\begin{aligned} \Phi_{5f}^{(1)} \otimes H^{(0)} = & \frac{\alpha_s C_f}{8\pi} \left[\frac{1}{\epsilon} + \ln \frac{4\pi\mu_f^2}{m_B^2 e^{\gamma_E}} + \ln r_1 - 2 \ln x_1 \right. \\ & \left. - (\ln \delta_1 - 2 \ln x_1 + \ln r_1)^2 - 2 (\ln \delta_1 - 2 \ln x_1 + \ln r_1) - \frac{\pi^2}{3} + 2 \right] H^{(0)}, \end{aligned} \quad (41)$$

$$\Phi_{5g}^{(1)} \otimes H^{(0)} = \frac{\alpha_s C_f}{8\pi} \left[(\ln \delta_1 - 2 \ln x_1 + \ln r_1)^2 - \frac{\pi^2}{3} \right] H^{(0)},$$

$$\left(\Phi_{5h}^{(1)} + \Phi_{5i}^{(1)} + \Phi_{5j}^{(1)} \right) \otimes H^{(0)} = \frac{\alpha_s C_f}{4\pi} \left[\frac{1}{\epsilon} + \ln \frac{4\pi\mu_f^2}{m_B^2 e^{\gamma_E}} - \ln \delta_{12} \right] H^{(0)}, \quad (42)$$

where the dimensionless parameter $r_1 = m_B^2/\xi_1^2$ is chosen small to obtain the simple results as above. Because the two propagators in the LO hard kernel $H^{(0)}$ are both relevant to x'_1 while only one is relevant to x'_2 , there exist three 5-point integrals as shown in Fig. 5(c,e,g) need to be calculated. The reducible subdiagrams Fig. 5(c) reproduced the double logarithm as the quark subdiagram Fig. 4(b). Difference between the effective heavy-quark field employed in the B meson wave function and the b quark field in the quark diagrams leads to different results in Fig. 4(b) and Fig. 5(c). It's found that the regulator $\ln m_g$ adopted to regularize the soft divergence in the reducible Fig. 5(a) will be canceled by the Fig. 2(a), while the regulators $\ln m_g$ in Fig. 5(d) and Fig. 5(e) cancels each other. The large double logarithms $(\ln \delta_1 - 2 \ln x_1 + \ln r_1)^2$ in Fig. 5(f) and Fig. 5(g) also cancel each other. So the other IR divergences are regulated only by $\ln \delta_1$ as the prediction because it's just the NLO correction to the incoming B meson wave function.

After summing all the $O(\alpha_s)$ contributions in Fig. 5, we obtain

$$\begin{aligned} \Phi_B^{(1)} \otimes H^{(0)} = & \frac{\alpha_s C_f}{4\pi} \left[\frac{1}{2} (4 + \ln r_1) \left(\frac{1}{\epsilon} + \ln \frac{4\pi\mu_f^2}{m_B^2 e^{\gamma_E}} \right) - \ln^2 \delta_1 \right. \\ & + \frac{1}{2} (-1 + 8 \ln x_1) \ln \delta_1 - \ln r_g - 4 \ln^2 x_1 + (1 - \ln r_1) \ln x_1 \\ & \left. - \frac{1}{2} \ln r_1 + \frac{1}{4} \ln^2 r_1 - \ln \delta_{12} - \frac{\pi^2}{3} \right] H^{(0)}. \end{aligned} \quad (43)$$

The convolution of $H^{(0)}$ and the $O(\alpha_s)$ outgoing pion meson wave function $\Phi_\pi^{(1)}$ over the integration variables x'_2 and k'_{2T} is

$$H^{(0)} \otimes \Phi_{\pi,P}^{(1)} \equiv \int dx'_2 d^2 \mathbf{k}'_{2T} H^{(0)}(x_1, \mathbf{k}_{1T}; x'_2, \mathbf{k}'_{2T}) \Phi_{\pi,P}^{(1)}(x'_2, \mathbf{k}'_{2T}; x_2, \mathbf{k}_{2T}). \quad (44)$$

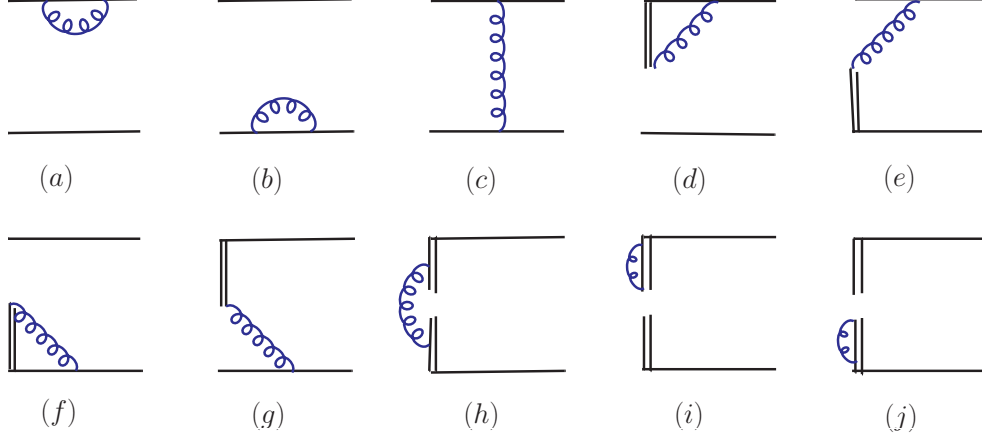


FIG. 6. $O(\alpha_s)$ diagrams for the π meson function.

The n_2 is mainly in n_+ component, and a very small minus component n_2^- is kept to avoid the LC singularity. Note that the sign of n_2^+ is positive as P_1^+ while the sign of n_2^- is arbitrary for convenience.

Fig. 6 collects all the NLO corrections to the outgoing pion wave function, and $r_2 = m_B^2/\xi_2^2$. The reducible subdiagrams Fig. 5(a,b,c) and Fig. 6(a,b,c) generate the same results as in the leading twist-2 case[15], while the results from the irreducible subdiagrams Fig. 5(d,e,f,g,h,i,j) and Fig. 6(d,e,f,g,h,i,j) in the twist-3 is half smaller than that in the leading twist-2, due to their different spin structures. The amplitude of the reducible Fig. 6(c), convoluted by the LO hard kernel $H^{(0)}$, reproduced the double logarithm $\ln \delta_1 \ln \delta_2$. There are no five-point integrals in $H^{(0)} \otimes \Phi^{(1)}$ because only one denominator in $H^{(0)}$ is relevant to x'_2 . Then the most complicated integrals involved here is the four-point integrations attached to Fig. 6(e,g). The double logarithm in $H^{(0)} \otimes \Phi_{8d}^{(1)}$, $H^{(0)} \otimes \Phi_{8e}^{(1)}$, $H^{(0)} \otimes \Phi_{8f}^{(1)}$ and $H^{(0)} \otimes \Phi_{8g}^{(1)}$ are also canceled. Only a double logarithm $\ln \delta_1 \ln \delta_2$, which would be canceled by the quark diagram Fig. 4(d), still left in the $H^{(0)} \otimes \Phi_{\pi,P}^{(1)}$.

The analytical results from Fig. 6 are listed in the following with μ_f being the factorization scale.

$$H^{(0)} \otimes \Phi_{6a}^{(1)} = -\frac{\alpha_s C_f}{8\pi} \left[\frac{1}{\epsilon} + \ln \frac{4\pi\mu_f^2}{m_B^2 e^{\gamma_E}} - \ln \delta_2 + 2 \right] H^{(0)}, \quad (45)$$

$$H^{(0)} \otimes \Phi_{6b}^{(1)} = -\frac{\alpha_s C_f}{8\pi} \left[\frac{1}{\epsilon} + \ln \frac{4\pi\mu_f^2}{m_B^2 e^{\gamma_E}} - \ln \delta_2 + 2 \right] H^{(0)}, \quad (46)$$

$$H^{(0)} \otimes \Phi_{6c}^{(1)} = -\frac{\alpha_s C_f}{2\pi} \left[\ln \frac{\delta_{12}}{\delta_1} \ln \frac{\delta_{12}}{\delta_2} + \frac{\pi^2}{3} \right] H^{(0)}, \quad (47)$$

$$H^{(0)} \otimes \Phi_{6d}^{(1)} = \frac{\alpha_s C_f}{8\pi} \left[\frac{1}{\epsilon} + \ln \frac{4\pi\mu_f^2}{m_B^2 e^{\gamma_E}} - \ln \delta_2 - (\ln r_2 + \ln \delta_2)^2 \right. \\ \left. - (\ln r_2 + \ln \delta_2) + 2 - \frac{\pi^2}{3} \right] H^{(0)}, \quad (48)$$

$$H^{(0)} \otimes \Phi_{6e}^{(1)} = \frac{\alpha_s C_f}{8\pi} \left[(\ln x_2 - \ln r_2 - \ln \delta_2)^2 + \pi^2 \right] H^{(0)}, \quad (49)$$

$$H^{(0)} \otimes \Phi_{6f}^{(1)} = \frac{\alpha_s C_f}{8\pi} \left[\frac{1}{\epsilon} + \ln \frac{4\pi\mu_f^2}{m_B^2 e^{\gamma_E}} - \ln \delta_2 - (2 \ln x_2 - \ln r_2 - \ln \delta_2)^2 \right. \\ \left. + (2 \ln x_2 - \ln r_2 - \ln \delta_2) + 2 - \frac{\pi^2}{3} \right] H^{(0)}, \quad (50)$$

$$H^{(0)} \otimes \Phi_{6g}^{(1)} = \frac{\alpha_s C_f}{8\pi} \left[(2 \ln x_2 - \ln r_2 - \ln \delta_2)^2 - \frac{\pi^2}{3} \right] H^{(0)}, \quad (51)$$

$$H^{(0)} \otimes (\Phi_{6h}^{(1)} + \Phi_{6i}^{(1)} + \Phi_{6j}^{(1)}) = \frac{\alpha_s C_f}{4\pi} \left[\frac{1}{\epsilon} + \ln \frac{4\pi\mu_f^2}{m_B^2 e^{\gamma_E}} - \ln \delta_{12} \right] H^{(0)}. \quad (52)$$

The total contributions from the convolution of the LO hard kernel and the NLO final pion meson wave function is obtained by summing all terms as given in above equations.

$$H^{(0)} \otimes \Phi_{\pi,P}^{(1)} = \frac{\alpha_s C_f}{4\pi} \left[\left(\frac{1}{\epsilon} + \ln \frac{4\pi\mu_f^2}{m_B^2 e^{\gamma_E}} \right) - 2 \ln \delta_1 \ln \delta_2 + 2 \ln \delta_{12} \ln \delta_1 \right. \\ \left. - (1 + \ln x_2 - 2 \ln \delta_{12}) \ln \delta_2 + \frac{1}{2} \ln^2(x_2) + (1 - \ln r_2) \ln x_2 \right. \\ \left. - \ln r_2 - \ln \delta_{12} - 2 \ln^2 \delta_{12} - \frac{2\pi^2}{3} \right] H^{(0)}. \quad (53)$$

C. NLO Hard Kernel

It's obvious that the UV poles are different in Eq. (43) and Eq. (53), since the former involves the effective heavy-quark field, instead of the b quark field. Then the B meson and pion meson wave functions exhibit different evolution as proved in Ref. [15]. The $\ln \mu_f$ term in Eq. (43) was partly absorbed into the B meson wave function, and partly to the B meson decay constant $f_B(\mu_f)$.

The IR-finite k_T dependent NLO hard kernel for the $B \rightarrow \pi$ transition form factor at twist-3 is extracted by taking the difference between the contributions from QCD quark diagrams and the contributions from effective diagrams [31].

$$H^{(1)}(x_1, \mathbf{k}_{1T}; x_2, \mathbf{k}_{2T}) = G^{(1)}(x_1, \mathbf{k}_{1T}; x_2, \mathbf{k}_{2T}) \\ - \int dx'_1 d^2 \mathbf{k}'_{1T} \Phi_B^{(1)}(x_1, \mathbf{k}_{1T}; x'_1, \mathbf{k}'_{1T}) H^{(0)}(x'_1, \mathbf{k}'_{1T}; x_2, \mathbf{k}_{2T}) \\ - \int dx'_2 d^2 \mathbf{k}'_{2T} H^{(0)}(x_1, \mathbf{k}_{1T}; x'_2, \mathbf{k}'_{2T}) \Phi_{\pi,P}^{(1)}(x'_2, \mathbf{k}'_{2T}; x_2, \mathbf{k}_{2T}). \quad (54)$$

The bare coupling constant α_s in Eq. (30,43,53) can be rewritten as

$$\alpha_s = \alpha_s(\mu_f) + \delta Z(\mu_f) \alpha_s(\mu_f), \quad (55)$$

in which the counterterm $\delta Z(\mu_f)$ is defined in the \overline{MS} scheme. Inserting Eq. (55) into Eqs. (18,30) and (43,53) regularizes the UV poles in Eq. (54) through the multiplication $\delta Z(\mu_f) H^{(0)}$, and then the UV poles in Eqs. (43,53) are regulated by the counterterm of the quark field and by an additional counterterm in the \overline{MS} scheme.

The NLO hard kernel $H^{(1)}$ for Fig. 1(b) at twist-3 is given by

$$\begin{aligned}
H^{(1)} = & \frac{\alpha_s(\mu_f)C_F}{4\pi} \left\{ \frac{21}{4} \ln \frac{\mu^2}{m_B^2} - \frac{1}{2}(6 + \ln r_1) \ln \frac{\mu_f^2}{m_B^2} - \frac{1}{16} \ln^2 x_1 - \frac{3}{8} \ln^2 x_2 \right. \\
& + \frac{9}{8} \ln x_1 \ln x_2 + \left(-\frac{33}{8} + \ln r_1 + \frac{15}{8} \ln \eta \right) \ln x_1 + \left(-\frac{25}{16} + \ln r_2 + \frac{9}{8} \ln \eta \right) \ln x_2 \\
& \left. + \frac{1}{2} \ln r_1 - \frac{1}{4} \ln^2 r_1 + \ln r_2 - \frac{9}{8} \ln \eta - \frac{1}{8} \ln^2 \eta + \frac{95\pi^2}{96} + \frac{273}{96} \right\} H^{(0)}. \quad (56)
\end{aligned}$$

The choice of the dimensionless scales ξ_1^2 and ξ_2^2 corresponds to a factorization scheme as discussed in the last subsection. The ξ_2^2 is fixed to m_B^2 and $\xi_1/m_B = 25$ is chosen in the numerical analysis to obtain the simplified results in Eqs. (39-42).

The additional double logarithm $\ln^2 x_1$ derived from the limit that the internal quark is on-shell due to the tiny momentum fraction x_1 should be considered. It's absorbed into the jet function $J(x_1)$ [18, 19]

$$J^{(1)} H^{(0)} = -\frac{1}{2} \frac{\alpha_s(\mu_f)C_F}{4\pi} \left[\ln^2(x_1) + \ln x_1 + \frac{\pi^2}{3} \right] H^{(0)}, \quad (57)$$

where the factor 1/2 reflects the different spin structures of the twist-3 and twist-2 cases. The NLO hard kernel from Eq. (56) turns into the following format after subtracting the jet function in Eq. (57)

$$\begin{aligned}
H^{(1)} & \rightarrow H^{(1)} - J^{(1)} H^{(0)} \\
& = \frac{\alpha_s(\mu_f)C_F}{4\pi} \left[\frac{21}{4} \ln \frac{\mu^2}{m_B^2} - \frac{1}{2}(6 + \ln r_1) \ln \frac{\mu_f^2}{m_B^2} + \frac{7}{16} \ln^2 x_1 - \frac{3}{8} \ln^2 x_2 \right. \\
& \quad + \frac{9}{8} \ln x_1 \ln x_2 + \left(-\frac{29}{8} + \ln r_1 + \frac{15}{8} \ln \eta \right) \ln x_1 + \left(-\frac{25}{16} + \ln r_2 + \frac{9}{8} \ln \eta \right) \ln x_2 \\
& \quad \left. + \frac{1}{2} \ln r_1 - \frac{1}{4} \ln^2 r_1 + \ln r_2 - \frac{9}{8} \ln \eta - \frac{1}{8} \ln^2 \eta + \frac{37\pi^2}{32} + \frac{91}{32} \right] H^{(0)} \\
& = F_{T3}^{(1)}(x_i, \mu, \mu_f, q^2) H^{(0)}, \quad (58)
\end{aligned}$$

where $r_i = m_B^2/\xi_i^2$, $\eta = 1 - q^2/m_B^2$. The IR-finite k_T dependent function $F_{T3}^{(1)}(x_i, \mu, \mu_f, q^2)$ in Eq. (58) describes the NLO twist-3 contribution to the $B \rightarrow \pi$ transition form factor $f^+(q^2)$ and $f^0(q^2)$ as defined in Eq. (1).

IV. NUMERICAL ANALYSIS

In this section, the $B \rightarrow \pi$ transition form factors will be evaluated numerically up to twist-3 by employing the k_T factorization theorem, and the comparative analysis is developed between the LO and NLO as well as between the twist-2 and twist-3 NLO corrections.

In the calculation, the following non-asymptotic pion distribution amplitudes (DAs) as given in Refs. [32, 33] will be used:

$$\begin{aligned}\phi_\pi^A(x) &= \frac{6f_\pi}{2\sqrt{2N_c}}x(1-x) \left[1 + a_2^\pi C_2^{\frac{3}{2}}(u) + a_4^\pi C_4^{\frac{3}{2}}(u) \right], \\ \phi_\pi^P(x) &= \frac{f_\pi}{2\sqrt{2N_c}} \left[1 + \left(30\eta_3 - \frac{5}{2}\rho_\pi^2 \right) C_2^{\frac{1}{2}}(u) - 3 \left(\eta_3\omega_3 + \frac{9}{20}\rho_\pi^2(1 + 6a_2^\pi) \right) C_4^{\frac{1}{2}}(u) \right], \\ \phi_\pi^T(x) &= \frac{f_\pi}{2\sqrt{2N_c}}(1-2x) \left[1 + 6 \left(5\eta_3 - \frac{1}{2}\eta_3\omega_3 - \frac{7}{20}\rho_\pi^2 - \frac{3}{5}\rho_\pi^2 a_2^\pi \right) (1 - 10x + 10x^2) \right] \quad (59)\end{aligned}$$

where $u = 2x - 1$, $m_\pi = 0.135$ GeV, $f_\pi = 0.13$ GeV, $m_0^\pi = 1.4$ GeV, and the Gegenbauer moments and Gegenbauer polynomials are adopted from Refs. [34, 35],

$$a_2^\pi = 0.25, \quad a_4^\pi = -0.015, \quad \rho_\pi = \frac{m_\pi}{m_0^\pi}, \quad \eta_3 = 0.015, \quad \omega_3 = -3.0, \quad (60)$$

$$\begin{aligned}C_2^{1/2} &= \frac{1}{2}(3u^2 - 1), \quad C_2^{3/2} = \frac{3}{2}(5u^2 - 1), \\ C_4^{1/2} &= \frac{1}{8}(3 - 30u^2 + 35u^4), \quad C_4^{3/2} = \frac{15}{8}(1 - 14u^2 + 21u^4), \quad (61)\end{aligned}$$

The B meson distribution amplitude widely used in the pQCD approach is of the form [21, 22]

$$\phi_B(x, b) = \frac{f_B}{2\sqrt{2N_c}} N_B x^2 (1-x)^2 \cdot \exp \left[-\frac{x^2 m_B^2}{2\omega_B^2} - \frac{1}{2}(\omega_B b)^2 \right], \quad (62)$$

where we have assumed that $\phi_B(x, b) = \phi_B^+(x, b) = \phi_B^-(x, b)$. The normalization condition of $\phi_B(x, b)$ is

$$\int_0^1 dx \phi_B(x, b=0) = \frac{f_B}{2\sqrt{2N_c}}, \quad (63)$$

with the mass $m_B = 5.28$ GeV, while the normalization constant $N_B = 100.921$ for $f_B = 0.21$ GeV and the fixed shape parameter $\omega_B = 0.40$.

The form factor $f^+(q^2)$ and $f^0(q^2)$ at full LO level can be written as [21]

$$\begin{aligned}f^+(q^2)|_{\text{LO}} &= 8\pi m_B^2 C_F \int dx_1 dx_2 \int b_1 db_1 b_2 db_2 \phi_B(x_1, b_1) \\ &\times \left\{ r_\pi \left[\phi_\pi^P(x_2) - \phi_\pi^T(x_2) \right] \cdot \alpha_s(t_1) \cdot e^{-S_{B\pi}(t_1)} \cdot S_t(x_2) \cdot h(x_1, x_2, b_1, b_2) \right. \\ &+ \left[(1 + x_2\eta) \phi_\pi^A(x_2) + 2r_\pi \left(\frac{1}{\eta} - x_2 \right) \phi_\pi^T(x_2) - 2x_2 r_\pi \phi_\pi^P(x_2) \right] \\ &\quad \cdot \alpha_s(t_1) \cdot e^{-S_{B\pi}(t_1)} \cdot S_t(x_2) \cdot h(x_1, x_2, b_1, b_2) \\ &\left. + 2r_\pi \phi_\pi^P(x_2) \cdot \alpha_s(t_2) \cdot e^{-S_{B\pi}(t_2)} \cdot S_t(x_1) \cdot h(x_2, x_1, b_2, b_1) \right\}, \quad (64)\end{aligned}$$

$$\begin{aligned}
f^0(q^2)|_{\text{LO}} = & 8\pi m_B^2 C_F \int dx_1 dx_2 \int b_1 db_1 b_2 db_2 \phi_B(x_1, b_1) \\
& \times \left\{ r_\pi (2 - \eta) [\phi_\pi^P(x_2) - \phi_\pi^T(x_2)] \cdot \alpha_s(t_1) \cdot e^{-S_{B\pi}(t_1)} \cdot S_t(x_2) \cdot h(x_1, x_2, b_1, b_2) \right. \\
& + [(1 + x_2\eta)\eta\phi_\pi^A(x_2) + 2r_\pi(1 - x_2\eta)\phi_\pi^T(x_2) - 2x_2\eta r_\pi\phi_\pi^P(x_2)] \\
& \quad \cdot \alpha_s(t_1) \cdot e^{-S_{B\pi}(t_1)} \cdot S_t(x_2) \cdot h(x_1, x_2, b_1, b_2) \\
& \left. + 2\eta r_\pi\phi_\pi^P(x_2) \cdot \alpha_s(t_2) \cdot e^{-S_{B\pi}(t_2)} \cdot S_t(x_1) \cdot h(x_2, x_1, b_2, b_1) \right\}, \tag{65}
\end{aligned}$$

where $r_\pi = m_0^\pi/m_B$, the term proportional to ϕ_π^A denotes the LO twist-2 contribution, while those proportional to ϕ_π^P and ϕ_π^T make up of the LO twist-3 contribution. The factor $\exp[-S_{B\pi}(t)]$ in Eqs. (64,65) contains the Sudakov logarithmic corrections and the renormalization group evolution effects of both the wave functions and the hard scattering amplitude with $S_{B\pi}(t) = S_B(t) + S_\pi(t)$, where

$$\begin{aligned}
S_B(t) &= s\left(x_1 \frac{m_B}{\sqrt{2}}, b_1\right) + \frac{5}{3} \int_{1/b_1}^t \frac{d\bar{\mu}}{\bar{\mu}} \gamma_q(\alpha_s(\bar{\mu})), \\
S_\pi(t) &= s\left(x_2 \frac{m_B}{\sqrt{2}}, b_2\right) + s\left((1 - x_2) \frac{m_B}{\sqrt{2}}, b_2\right) + 2 \int_{1/b_2}^t \frac{d\bar{\mu}}{\bar{\mu}} \gamma_q(\alpha_s(\bar{\mu})), \tag{66}
\end{aligned}$$

with the quark anomalous dimension $\gamma_q = -\alpha_s/\pi$. The functions $s(Q, b)$ are defined by [21]

$$\begin{aligned}
s(Q, b) &= \frac{A^{(1)}}{2\beta_1} \hat{q} \ln\left(\frac{\hat{q}}{\hat{b}}\right) - \frac{A^{(1)}}{2\beta_1} (\hat{q} - \hat{b}) + \frac{A^{(2)}}{4\beta_1^2} \left(\frac{\hat{q}}{\hat{b}} - 1\right) \\
&\quad - \left[\frac{A^{(2)}}{4\beta_1^2} - \frac{A^{(1)}}{4\beta_1} \ln\left(\frac{e^{2\gamma_E} - 1}{2}\right) \right] \ln\left(\frac{\hat{q}}{\hat{b}}\right) \\
&\quad + \frac{A^{(1)}\beta_2}{4\beta_1^3} \hat{q} \left[\frac{\ln(2\hat{q}) + 1}{\hat{q}} - \frac{\ln(2\hat{b}) + 1}{\hat{b}} \right] + \frac{A^{(1)}\beta_2}{8\beta_1^3} [\ln^2(2\hat{q}) - \ln^2(2\hat{b})], \tag{67}
\end{aligned}$$

where the variables are defined by $\hat{q} = \ln[Q/(\sqrt{2}\Lambda)]$, $\hat{b} = \ln[1/(b\Lambda)]$, and the coefficients $A^{(i)}$ and β_i are

$$\begin{aligned}
\beta_1 &= \frac{33 - 2n_f}{12}, \quad \beta_2 = \frac{153 - 19n_f}{24}, \quad A^{(1)} = \frac{4}{3}, \\
A^{(2)} &= \frac{67}{9} - \frac{\pi^2}{3} - \frac{10n_f}{27} + \frac{8}{3}\beta_1 \ln(e^{\gamma_E}/2). \tag{68}
\end{aligned}$$

Here, n_f is the number of the quark flavors, and the γ_E is the Euler constant. The hard scales t_i in the equations of this work are chosen as the largest scale of the virtuality of the internal particles in the hard b -quark decay diagram,

$$t_1 = \max\{\sqrt{x_2\eta}m_B, 1/b_1, 1/b_2\}, \quad t_2 = \max\{\sqrt{x_1\eta}m_B, 1/b_1, 1/b_2\}. \tag{69}$$

The function $S_t(x)$ in Eqs. (64,65) is the threshold resummation factor that is adopted from Ref. [21]:

$$S_t(x) = \frac{2^{1+2c}\Gamma(3/2+c)}{\sqrt{\pi}\Gamma(1+c)} [x(1-x)]^c, \tag{70}$$

where we set the parameter $c = 0.3$. The hard functions $h(x_1, x_2, b_1, b_2)$ come from the Fourier transform of the hard kernel and can be written as [14]

$$h(x_1, x_2, b_1, b_2) = K_0(\sqrt{x_1 x_2 \eta} m_B b_1) \left[\theta(b_1 - b_2) I_0(\sqrt{x_2 \eta} m_B b_2) K_0(\sqrt{x_2 \eta} m_B b_1) + \theta(b_2 - b_1) I_0(\sqrt{x_2 \eta} m_B b_1) K_0(\sqrt{x_2 \eta} m_B b_2) \right], \quad (71)$$

where I_0 and K_0 are the modified Bessel functions.

Before taking the NLO twist-3 contributions into account, we have to make a choice for the scale μ and μ_f , and try to minimize the NLO correction to the form factor. Following Ref. [15], we also set $\mu_f = t$ with $t = t_1$ or t_2 , the hard scale specified in the pQCD approach as given in Eq. (69), which is the largest energy scale in Fig. 1(a) or 1(b) respectively. The renormalization scale μ is chosen to diminish all the single-logarithm and constant terms in the NLO hard kernel (58) [15]:

$$t_s(\mu_f) = \left\{ \text{Exp} \left[c1 + \left(-\frac{9}{4} + \frac{1}{2} \ln r_1 \right) \ln \frac{\mu_f^2}{m_B^2} x_1^{c2} x_2^{c3} \right] \right\}^{2/21} \cdot \mu_f, \quad (72)$$

with the coefficients

$$\begin{aligned} c1 &= -\left(\frac{1}{2} - \frac{1}{4} \ln r_1 \right) \ln r_1 + \left(\frac{9}{8} + \frac{1}{8} \ln \eta \right) \ln \eta - \frac{379}{32} - \frac{167\pi^2}{96}, \\ c2 &= \frac{29}{8} - \ln r_1 - \frac{15}{8} \ln \eta, \\ c3 &= \frac{25}{16} - \frac{9}{8} \ln \eta, \end{aligned} \quad (73)$$

based on our calculation.

When the NLO twist-2 and NLO twist-3 contributions to the $B \rightarrow \pi$ transition form factors are taken into account, the pQCD predictions for the two form factors at full NLO level are of the form

$$\begin{aligned} f^+(q^2)|_{\text{NLO}} &= 8\pi m_B^2 C_F \int dx_1 dx_2 \int b_1 db_1 b_2 db_2 \phi_B(x_1, b_1) \\ &\times \left\{ r_\pi [\phi_\pi^P(x_2) - \phi_\pi^T(x_2)] \cdot \alpha_s(t_1) \cdot e^{-S_{B\pi}(t_1)} \cdot S_t(x_2) \cdot h(x_1, x_2, b_1, b_2) \right. \\ &+ \left[(1 + x_2 \eta) \left(1 + F_{T2}^{(1)}(x_i, t, q^2) \right) \phi_\pi^A(x_2) + 2r_\pi \left(\frac{1}{\eta} - x_2 \right) \phi_\pi^T(x_2) - 2x_2 r_\pi \phi_\pi^P(x_2) \right] \\ &\quad \cdot \alpha_s(t_1) \cdot e^{-S_{B\pi}(t_1)} \cdot S_t(x_2) \cdot h(x_1, x_2, b_1, b_2) \\ &\left. + 2r_\pi \phi_\pi^P(x_2) \left(1 + F_{T3}^{(1)}(x_i, t, q^2) \right) \cdot \alpha_s(t_2) \cdot e^{-S_{B\pi}(t_2)} \cdot S_t(x_1) \cdot h(x_2, x_1, b_2, b_1) \right\}, \quad (74) \end{aligned}$$

$$\begin{aligned}
f^0(q^2)|_{\text{NLO}} = & 8\pi m_B^2 C_F \int dx_1 dx_2 \int b_1 db_1 b_2 db_2 \phi_B(x_1, b_1) \\
& \times \left\{ r_\pi (2 - \eta) [\phi_\pi^P(x_2) - \phi_\pi^T(x_2)] \cdot \alpha_s(t_1) \cdot e^{-S_{B\pi}(t_1)} \cdot S_t(x_2) \cdot h(x_1, x_2, b_1, b_2) \right. \\
& + \left[(1 + x_2 \eta) \left(1 + F_{\text{T2}}^{(1)}(x_i, t, q^2) \right) \eta \phi_\pi^A(x_2) + 2r_\pi (1 - x_2 \eta) \phi_\pi^T(x_2) - 2x_2 \eta r_\pi \phi_\pi^P(x_2) \right] \\
& \quad \cdot \alpha_s(t_1) \cdot e^{-S_{B\pi}(t_1)} \cdot S_t(x_2) \cdot h(x_1, x_2, b_1, b_2) \\
& \left. + 2\eta r_\pi \left(1 + F_{\text{T3}}^{(1)}(x_i, t, q^2) \right) \phi_\pi^P(x_2) \cdot \alpha_s(t_2) \cdot e^{-S_{B\pi}(t_2)} \cdot S_t(x_1) \cdot h(x_2, x_1, b_2, b_1) \right\}, \quad (75)
\end{aligned}$$

where the factor $F_{\text{T2}}^{(1)}(x_i, t, q^2)$ describes the NLO twist-2 contribution as given in Ref. [15]

$$\begin{aligned}
F_{\text{T2}}^{(1)}(x_i, t, q^2) = & \frac{\alpha_s(\mu_f) C_F}{4\pi} \left[\frac{21}{4} \ln \frac{\mu^2}{m_B^2} - \left(\frac{13}{2} + \ln r_1 \right) \ln \frac{\mu_f^2}{m_B^2} + \frac{7}{16} \ln^2(x_1 x_2) + \frac{1}{8} \ln^2 x_1 \right. \\
& + \frac{1}{4} \ln x_1 \ln x_2 + \left(-\frac{1}{4} + 2 \ln r_1 + \frac{7}{8} \ln \eta \right) \ln x_1 + \left(-\frac{3}{2} + \frac{7}{8} \ln \eta \right) \ln x_2 \\
& \left. + \frac{15}{4} \ln \eta - \frac{7}{16} \ln^2 \eta + \frac{3}{2} \ln^2 r_1 - \ln r_1 + \frac{101\pi^2}{48} + \frac{219}{16} \right]. \quad (76)
\end{aligned}$$

The factor $F_{\text{T3}}^{(1)}(x_i, t, q^2)$ in Eqs. (74,75) denotes the NLO twist-3 contribution as defined in Eq. (58):

$$\begin{aligned}
F_{\text{T3}}^{(1)}(x_i, t, q^2) = & \frac{\alpha_s(\mu_f) C_F}{4\pi} \left[\frac{21}{4} \ln \frac{\mu^2}{m_B^2} - \frac{1}{2} (6 + \ln r_1) \ln \frac{\mu_f^2}{m_B^2} + \frac{7}{16} \ln^2 x_1 - \frac{3}{8} \ln^2 x_2 \right. \\
& + \frac{9}{8} \ln x_1 \ln x_2 + \left(-\frac{29}{8} + \ln r_1 + \frac{15}{8} \ln \eta \right) \ln x_1 + \left(-\frac{25}{16} + \ln r_2 + \frac{9}{8} \ln \eta \right) \ln x_2 \\
& \left. + \frac{1}{2} \ln r_1 - \frac{1}{4} \ln^2 r_1 + \ln r_2 - \frac{9}{8} \ln \eta - \frac{1}{8} \ln^2 \eta + \frac{37\pi^2}{32} + \frac{91}{32} \right]. \quad (77)
\end{aligned}$$

The q^2 -dependence of the form factor $f^+(q^2)$ and $f^0(q^2)$ in the k_T factorization up to NLO are shown in Fig. 7 and Fig. 8. In order to show and compare directly the relative strength of the contributions from different sources, we also list the pQCD predictions for the values of $f^+(q^2)$ and $f^0(q^2)$ in Table I, assuming $\omega_B = 0.40$, $c = 0.3$ and $q^2 = (0, 1, 3, 5, 7, 10, 12)$ GeV². In Table I, the label ‘‘LO’’, ‘‘NLO-T2’’, ‘‘NLO-T3’’, and ‘‘NLO’’ mean the full LO contribution (LO twist-2 plus LO twist-3), the NLO twist-2 part only, the NLO twist-3 part only, and the total contribution at the NLO level (full LO contribution plus both NLO twist-2 and NLO twist-3 ones), respectively. In Table II, for the cases of $f^+(q^2)$ with $q^2 = (0, 5, 10)$ respectively, we show the pQCD predictions for various contributions to $f^+(q^2)$ from different sources: the LO twist-2, LO twist-3, NLO twist-2, NLO twist-3, and finally the total contribution at the NLO level. We also define the ratios $R_i = f_i^+(q^2)/f_{\text{LO}}^+(q^2)$ to measure the relative percentage of different contributions with respect to the full LO contribution.

From the curves in Fig. 7 and Fig. 8 and the numerical results in Table I and II, one can have the following observations:

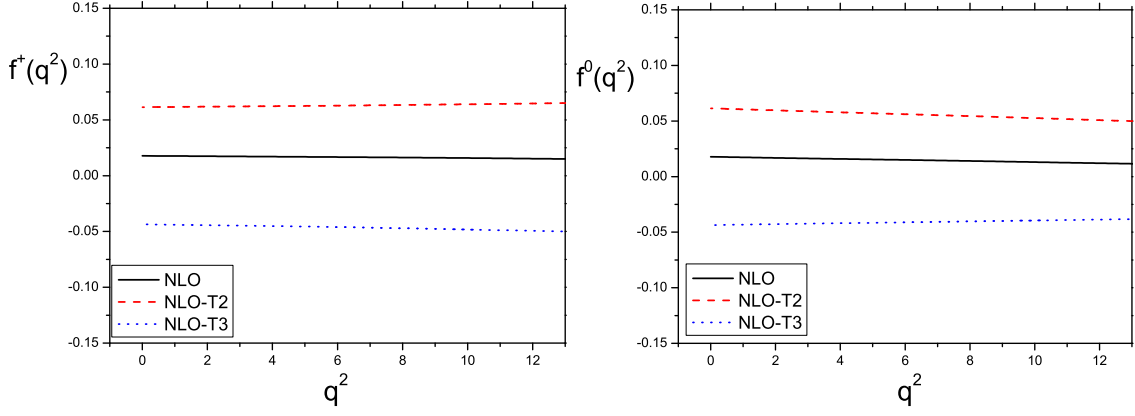


FIG. 7. The NLO twist-2 contribution (dashed-curve), the NLO twist-3 contribution (dots-curve), and the total NLO contribution (the solid curve) for $0 \leq q^2 \leq 12 \text{ GeV}^2$, and setting $\mu_f = t$ and $\mu = t_s(\mu_f)$ as given in Eqs. (69,72).

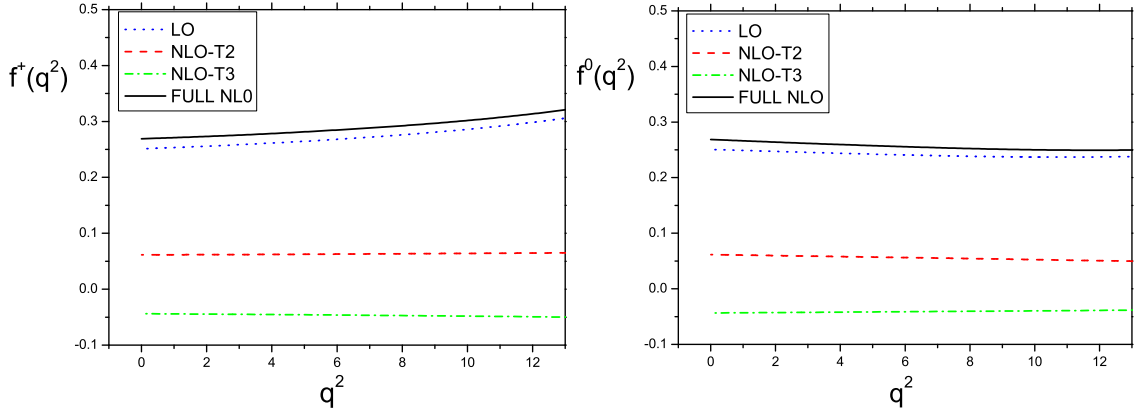


FIG. 8. The pQCD predictions for the form factor $f^+(q^2)$ and $f^0(q^2)$, assuming $\omega_B = 0.4$ and $c = 0.3$, and setting $\mu_f = t$ and $\mu = t_s(\mu_f)$. The left (right) diagram shows the q^2 -dependence of the form factor, with the inclusion of the full LO contribution (dots-curve), the NLO twist-2 contribution only (dashed-curve), the NLO twist-3 one only (the dot-dashed curve), and finally the total contribution at NLO level (the solid curve).

- (i) The NLO corrections at twist-2 and twist-3 are both under control, about 20% of the full LO contributions. The reason is that the end-point region of x_1 is strongly suppressed and the large double logarithm $\ln^2 x_1$ in $H^{(1)}$ don't bring the dominant contribution in the NLO corrections at both twists.
- (ii) From Fig. 7 and Table I and II, one can see that the NLO twist-2 and NLO twist-3 contributions are similar in size but have an opposite sign, which leads to a strong cancelation between NLO twist-2 and NLO twist-3 contributions and consequently results in a small total NLO contribution, as illustrated explicitly in Fig. 8. For the case of $f^+(0)$, for example, the LO twist-2 contribution is roughly half of the LO twist-3 part: 34% and 66% of the full LO contribution respectively, while the NLO twist-2 contribution can provide a $\sim 24\%$ enhancement to the LO prediction, but the NLO twist-3 part can provide a $\sim 17.5\%$ decrease for the LO one. The total NLO contribution results in, consequently, a 7% enhancement to the LO $f^+(0)$ only.
- (iii) Since the pQCD calculation for the form factors is reliable only at low q^2 region, we there-

TABLE I. The pQCD predictions for the values of $f^+(q^2)$ and $f^0(q^2)$ for $\omega_B = 0.40$ and $c = 0.3$, and assuming $q^2 = (0, 1, 3, 5, 7, 10, 12)$ GeV². The label LO, NLO-T2, NLO-T3, and NLO means the full LO contribution, the NLO twist-2 part only, the NLO twist-3 part only, and total contribution at NLO level: full LO plus both NLO twist-2 and twist-3 ones, respectively.

$f^+(q^2)$	0	1	3	5	7	10	12
LO	0.251	0.254	0.257	0.266	0.275	0.285	0.301
NLO-T2	0.061	0.061	0.062	0.063	0.063	0.064	0.064
NLO-T3	-0.043	-0.044	-0.044	-0.045	-0.046	-0.047	-0.048
NLO	0.269	0.271	0.275	0.284	0.294	0.302	0.317
$f^0(q^2)$	0	1	3	5	7	10	12
LO	0.251	0.248	0.246	0.243	0.239	0.237	0.236
NLO-T2	0.061	0.060	0.059	0.057	0.055	0.052	0.051
NLO-T3	-0.043	-0.043	-0.042	-0.042	-0.041	-0.040	-0.039
NLO	0.269	0.265	0.263	0.258	0.253	0.249	0.248

TABLE II. The pQCD predictions for various contributions $f_i^+(q^2)$ for $q^2 = (0, 5, 10)$ and their ratios $R_i(q^2) = f_i^+(q^2)/f_{LO}^+(q^2)$.

Source	$f_i(0)$	$R_i(0)$	$f_i(5)$	$R_i(5)$	$f_i(10)$	$R_i(10)$
LO	0.251	100%	0.266	100%	0.285	100%
LO-T2	0.086	34.3%	0.084	31.6%	0.082	28.8%
NLO-T2	0.061	24.3%	0.063	23.7%	0.064	22.5%
LO-T3	0.165	65.7%	0.182	68.4%	0.203	71.2%
NLO-T3	-0.044	-17.1%	-0.045	-16.9%	-0.047	-16.5%
NLO	0.269	107.2%	0.284	106.8%	0.302	106.0%

fore show the pQCD predictions for $f^+(q^2)$ and $f^0(q^2)$ in the region of $0 \leq q^2 \leq 12$ GeV² only. One can see from Figs. 7 and 8 that the pQCD predictions for the two form factors have a weak q^2 -dependence: a 24% (22%) increase for the LO (NLO) prediction for $f^+(q^2)$, but a 8% (6%) decrease for the LO (NLO) prediction for $f^0(q^2)$, for the variation of q^2 from $q^2 = 0$ to $q^2 = 12$ GeV².

In our numerical calculations, the main theoretical errors come from the uncertainties of the input parameters $\omega_B = 0.40 \pm 0.04$, $a_2 = 0.25 \pm 0.15$ and $m_0^\pi = 1.4 \pm 0.2$ GeV. In Fig. 9, we show the central values and the theoretical uncertainties of the NLO pQCD predictions for both form factors $f^+(q^2)$ and $f^0(q^2)$ of $B \rightarrow \pi$ transition, where the theoretical errors from different sources are added in quadrature. For the case of $q^2 = 0$ ($\eta = 1$), we find numerically that

$$\begin{aligned}
 f^+(0) &= f^0(0) = 0.269^{+0.042}_{-0.035}(w_B)^{+0.028}_{-0.029}(a_2^\pi) \pm 0.020(m_0^\pi) \\
 &= 0.269^{+0.054}_{-0.050}.
 \end{aligned} \tag{78}$$

It is easy to see that the total theoretical error of the NLO pQCD prediction for $f^{+,0}(0)$ is about

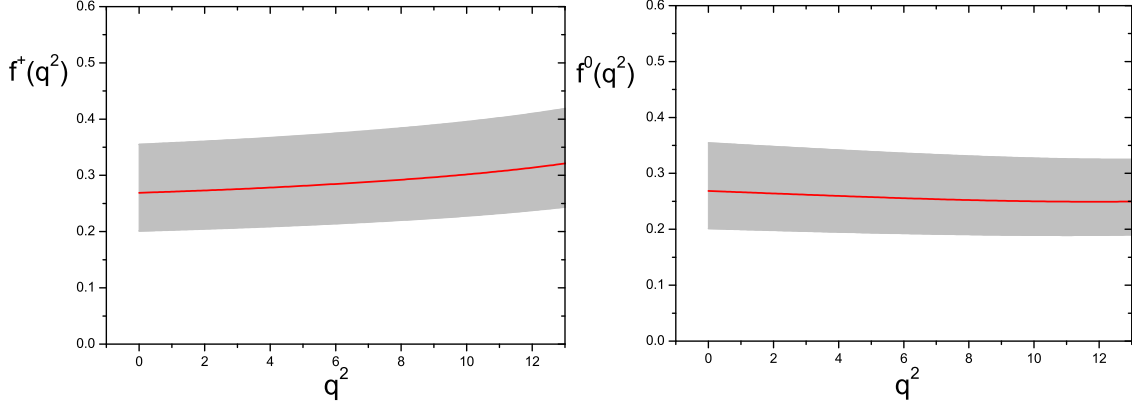


FIG. 9. Theoretical uncertainties of the $B \rightarrow \pi$ transition form factor with the choice $\mu_f = t$ and $\mu = t_s(\mu_f)$ in the range of $0 \leq q^2 \leq 12 \text{ GeV}^2$.

20% of its central value, and keep stable for the whole range of $0 \leq q^2 \leq 12 \text{ GeV}^2$, as illustrated in Fig. 9.

V. SUMMARY

In this paper, by employing the k_T factorization theorem, we calculated the NLO twist-3 contribution to the form factors $f^+(q^2)$ and $f^0(q^2)$ of the $B \rightarrow \pi$ transition.

The UV divergences are renormalized into the coupling constants, decay constant and quark fields. Both the soft and collinear divergences in the NLO QCD quark diagrams and in the NLO effective diagrams for meson wave functions are regulated by the off-shell momentum k_{iT}^2 of the light quark. The heavy b quark is protected on-shell to treat it as the standard effective heavy quark field in the k_T factorization theorem, and then the soft gluon radiated by the b quark can be regularized by the gluon mass m_g . With the reasonable choice of $\xi_2^2 = m_B^2$, only the NLO corrections of the B meson function develop an additional double logarithm $\ln^2 r_1$, with $r_1 = \xi_1^2/m_B^2$. And then the resummation technique is implemented to minimize the scheme dependence from the different choice of ξ_1^2 .

The cancelation of the IR divergences between the QCD quark diagrams and the effective diagrams for the meson wave functions at twist-3, in cooperation with the cancelation at the leading twist, verifies the validity of the k_T factorization for the $B \rightarrow \pi l^- \bar{\nu}_l$ semileptonic decays at the NLO level. The large double logarithm $\ln^2 x_1$ in the NLO hard kernel is resummed to result in the Sudakov factor, while the single logarithms and constant terms in the NLO hard kernel are all diminished by the choice of the scale μ and μ_f . We have demonstrated explicitly that the NLO corrections are under control.

From our analytical and numerical evaluations, we find that there is a strong cancelation between the NLO twist-2 and NLO twist-3 contribution to the form factors $f^{+,0}(q^2)$ of $B \rightarrow \pi$ transition. For the case of $f^+(0)$, for example, the NLO twist-2 contribution provides roughly 24% enhancement to the full LO one, but the NLO twist-3 contribution makes a 17.5% decrease for the full LO result. The total NLO contribution results in a 7% enhancement to the LO pQCD predictions, which is small and stable for the whole range of $0 \leq q^2 \leq 12 \text{ GeV}^2$.

ACKNOWLEDGMENTS

The authors would like to thank H.N. Li, Y.L. Shen, W.F. Wang and X. Liu for valuable discussions. This work is supported by the National Natural Science Foundation of China under Grant No.11235005, 11228512 and 11375208; and by the Project on Graduate Students Education and Innovation of Jiangsu Province under Grant No. CXZZ13-0391.

-
- [1] J. Botts and G. Sterman, **Nucl. Phys. B325**, 62 (1989); H.N. Li and G. Sterman, **Nucl. Phys. B381**, 129 (1992); T. Huang and Q.X. Shen, **Z. Phys. C50**, 139 (1991); F.G. Cao, T. Huang and C.W. Luo, **Phys. Rev. D52**, 5358(1995).
 - [2] J.C. Collins and R.K. Ellis, **Nucl. Phys. B360**, 3 (1991).
 - [3] H.N. Li and H.L. Yu, **Phys. Rev. Lett. 74**, 4388 (1995); H.N. Li and H.L. Yu, **Phys. Lett. B353**, 301 (1995); H.N. Li and H.L. Yu, **Phys. Rev. D53**, 2480 (1996).
 - [4] G.P. Lepage and S.J. Brodsky, **Phys. Lett. B87**, 359(1979).
 - [5] G.P. Lepage and S.J. Brodsky, **Phys. Rev. D22**, 2157(1980).
 - [6] A.V. Efremov and A.V. Radyushkin, **Phys. Lett. B94**, 245(1980).
 - [7] G. Sterman, An Intriduction to Quantum Field Theory, Cambridge University Press, Cambridge, England, 1993.
 - [8] M. Beneke and Th. Feldmann, **Nucl. Phys. B685**, 249 (2004).
 - [9] Y.Y. Keum, H.N. Li and A.I.Sanda, **Phys. Lett. B504**, 6 (2001), **Phys. Rev. D63**, 054008 (2001).
 - [10] C.D. Lü, K. Ukai and M.Z. Yang, **Phys. Rev. D63**, 074009 (2001). C.D. Lü and M.Z. Yang, **Eur. Phys. J. C28**, 515 (2003); H. Kawamura, J. Kodaira, C.F. Qiao and K.Tanaka, **Phys. Lett. B523**, 111 (2001).
 - [11] J.P. Ralston and B. Pire, **Phys. Rev. Lett. 65**, 2343 (1990).
 - [12] H.N. Li, **Prog. part. & Nucl.Phys. 51**, 85 (2003).
 - [13] S.Nandi and H.N. Li, **Phys. Rev. D76**, 034008 (2007).
 - [14] H.N. Li, Y.L. Shen, Y.M. Wang and H.Zou, **Phys. Rev. D83**, 054029(2011).
 - [15] H.N. Li, Y.L. Shen, Y.M. Wang, **Phys. Rev. D85**, 074004 (2012).
 - [16] H.N. Li, Y.L. Shen and Y.M. Wang, **J. High Energy Phys. 1401**, 004 (2014).
 - [17] S. Cheng, Y.Y. Fan, and Z.J. Xiao, **Phys. Rev. D89**, (2014) in press; arXiv:1401.5118[hep-ph].
 - [18] H.N. Li, **Phys. Rev. D66**, 094010 (2002).
 - [19] H.N. Li, **Phys. Lett. B555**, 197 (2003).
 - [20] M. Beneke and Th. Feldmann, **Nucl. Phys. B592**, 3 (2001).
 - [21] T. Kurimoto, H.N. Li, and A.I. Sanda, **Phys. Rev. D65**, 014007 (2001).
 - [22] C.D. Lü and M.Z. Yang, **Eur. Phys. J. C23**, 275 (2002).
 - [23] W. Siegel, **Phys. Lett. B84**, 193 (1979).
 - [24] H.N. Li and H.S. Liao, **Phys. Rev. D70**, 074030 (2004).
 - [25] H.N. Li, **Phys. Rev. D64**, 014019 (2001).
 - [26] M. Nagashima and H.N. Li, **Eur. Phys. J. C40**, 395 (2005).
 - [27] X. Ji and F. Yuan, **Phys. Lett. B543**, 66 (2002).
 - [28] J.C. Collins, **Acta. Phys. Polon. B34**, 3103 (2003).
 - [29] J.P. Ma and Q. Wang, **J. High Energy Phys. 0601**, 067 (2006); **Phys. Lett. B642**, 232 (2006).
 - [30] H.N. Li, Y.L. Shen and Y.M. Wang, **J. High Energy Phys. 1401**, 004(2014).
 - [31] M. Nagashima and H.N. Li, **Phys. Rev. D67**, 034001 (2003).

- [32] V.M. Braun and I.E. Filyanov, **Z. Phys. C48**, 239 (1990).
- [33] P. Ball, **J. High Energy Phys.** **9901**, 010 (1999).
- [34] P. Ball and R. Zwicky, **Phys. Rev. D71**, 014015 (2005).
- [35] P. Ball, V.M.Braun and A.Lenz, **J. High Energy Phys.** **0605**, 004 (2006), P. Ball, V.M. Braun, Y. Koike, and K. Tanaka, **Nucl. Phys. B529**, 323 (1998), P. Ball, **J. High Energy Phys.** 9809 (1998) 005.